NASA TECHNICAL NOTE

NASA TN D-7813

NASA TN D-7813

CALCULATION OF THE TWIST DISTRIBUTION OF WINGS DESIGNED FOR CRUISE AT TRANSONIC SPEEDS

by Michael J. Mann

Langley Research Center
Hampton, Va. 23665

NATIONAL AERONAUTICS AND SPACE ADMINISTRATION • WASHINGTON, D. C. • DECEMBER 1974

1. Report No.	2. Government Accession No.	3. Recipient's Catalog No.
NASA TN D-7813		

4. Title and Subtitle	5. Report Date
CALCULATION OF THE TWIST DISTRIBUTION OF WINGS DESIGNED FOR CRUISE AT TRANSONIC SPEEDS	December 1974
	6. Performing Organization Code
7. Author(s)	8. Performing Organization Report No.
Michael J. Mann	L-9832
	10. Work Unit No.
9. Performing Organization Name and Address	505-06-14-01
NASA Langley Research Center Hampton, Va. 23665	11. Contract or Grant No.
	13. Type of Report and Period Covered
12. Sponsoring Agency Name and Address	Technical Note
National Aeronautics and Space Administration Washington, D.C. 20546	14. Sponsoring Agency Code

15. Supplementary Notes

16. Abstract

The use of linear theory in calculating the twist distribution of a wing designed for cruise at supercritical speeds is justified on the basis of the transonic equivalence rule. A modified version of Multhopp's subsonic lifting-surface theory has been used to calculate the twist distribution. The lifting-surface theory is compared with both slender-wing theory and experimental results. A study is also made of the effect of wing sweep on the twist distribution required to maintain an elliptic span load at cruise conditions. The important parameters used in establishing this twist distribution are identified.

17. Key Words (Suggested by Author(s))	18. Distribution Statement
Wing twist Sonic aircraft Aircraft design Transonic aircraft	Unclassified – Unlimited STAR Category 01

19. Security Classif. (of this report)	20. Security Classif. (of this page)	21. No. of Pages	22. Price*
Unclassified	Unclassified	23	$3.25

*For sale by the National Technical Information Service, Springfield, Virginia 22151

CALCULATION OF THE TWIST DISTRIBUTION OF WINGS DESIGNED FOR CRUISE AT TRANSONIC SPEEDS

By Michael J. Mann
Langley Research Center

SUMMARY

The use of linear theory in calculating the twist distribution of a wing designed for cruise at supercritical speeds is justified on the basis of the transonic equivalence rule. A modified version of Multhopp's subsonic lifting-surface theory has been used to calculate the twist distribution. The lifting-surface theory is compared with both slender-wing theory and experimental results. A study is also made of the effect of wing sweep on the twist distribution required to maintain an elliptic span load at cruise conditions. The important parameters used in establishing this twist distribution are identified.

INTRODUCTION

Extensive aerodynamic research is currently being carried out in the area of transonic flight. The development of the National Aeronautics and Space Administration supercritical airfoil (ref. 1) has opened the possibility of speed increases and weight reduction in transport aircraft. With this airfoil, it may also be possible to improve the maneuvering capability of fighter aircraft operating at high lift in the transonic range, if proper account is taken of the low aspect ratio and high sweep of these aircraft.

The transonic technology developments which have occurred to date have relied almost exclusively on wind tunnel and other experimental techniques. Theoretical methods of calculating a transonic inviscid flow have largely been limited to two-dimensional solutions and to an endless variety of adaptations of three-dimensional linear solutions.

Bailey and Steger (ref. 2) and Ballhaus and Bailey (ref. 3) have developed numerical methods for solving the transonic small perturbation equation on three-dimensional lifting wings. The results of these methods show good agreement with other theoretical solutions and experimental data.

Slender-body theory has been used by Spreiter and Stahara (ref. 4) to study transonic lifting wing bodies at angles of attack where the flow is thickness dominated. The form of the equivalence rule discussed relates the lifting wing-body flow to the axisymmetric flow on a body of revolution having the same longitudinal distribution of cross-sectional area. (See also chapters 6 and 12 of ref. 5.) Some experimental verification of the theory was obtained.

Using the method of matched asymptotic expansions and approximations from slender-body and slender-wing theory, Barnwell (ref. 6) and Cheng and Hafez (ref. 7) have extended the theory of transonic lifting wing bodies to larger angles of attack. At larger angles of attack the effects of lift are comparable to, or dominate, the effects of thickness. The equivalence rule then relates the outer flow about a wing body to the axisymmetric flow about a body of revolution whose cross section depends both on the geometrical cross section of the original body and on the longitudinal lift distribution.

The design of minimum drag wings for transonic aircraft requires that the effects of the fuselage be taken into account. Near sonic speeds there is a strong interaction between the wing and fuselage. Small changes in the fuselage shape affect the strength of the shock waves, which in turn affects the performance of the wing. Aside from local effects, the equivalence rule itself shows that the fuselage and the lift distribution affect the overall area distribution. Presumably, the overall area distribution determines the shape for minimum drag configurations (local effects being considered). Hence, the slender-body theories may be useful for the design of minimum drag wings for transonic aircraft. However, these theories need experimental verification and further development.

Owing to the lack of a suitable transonic theory, linear theory is used for transonic design work under some conditions. Lock and Rogers (ref. 8) use linear theory in designing transonic wing bodies (moderate wing taper) so that the isobars on the wing are essentially straight. The concept has been experimentally verified by Lock (ref. 9) for conditions where the local Mach number normal to the isobars is less than 1.0 over most of the wing. A quasi-two-dimensional flow (independent of span location except at center-line kink and wing tips) without shock waves was obtained for the wing. There is no rigorous justification for this use of linear theory; however, theory shows that the flow over an infinite swept cylinder changes from elliptic to hyperbolic when the normal component of the Mach number exceeds 1.0 at any point in the flow.[1] Since the lift coefficients necessary in practice may be high enough so that some supercritical flow and shock waves exist on the wing, this design procedure may not always be practical.

The purpose of the present study is to justify the use of linear (subsonic lifting surface) theory for calculating the twist distribution required to maintain an elliptic span load at transonic cruise conditions. The justification for this use of linear theory is made on the basis of the transonic equivalence rule. The results are verified by comparison with experimental data and slender-wing theory. The effect of wing sweep on the required twist distribution is also investigated. The portion of the transonic range studied consists of speeds up to and including sonic free-stream Mach number.

---

[1]An infinite swept cylinder produces cylindrical pressure wavelets which propagate in a direction normal to the cylinder. These wavelets can only coalesce to form a shock wave when the normal component of the Mach number exceeds one.

SYMBOLS

Values are presented in both SI Units and U.S. Customary Units. The measurements and calculations were made in U.S. Customary Units.

$A^j(x,y,\eta)$ influence coefficient matrix elements, m^{-1} (ft^{-1}) (see eq. (6))

b wing span, m (ft)

C_L wing lift coefficient, $\frac{\text{Wing lift}}{q_\infty S}$

$C_{L,N}$ C_L based on V_N, see equation (10)

ΔC_p pressure loading, $\frac{p_{lower} - p_{upper}}{q_\infty}$

c local streamwise wing chord, m (ft)

c_{av} average chord, S/b, m (ft)

c_l section lift coefficient, $\frac{\text{Local chord load}}{q_\infty c}$

M_N component of M_∞ defined by equation (9)

M_∞ free-stream Mach number

N number of pressure modes is denoted by N + 1

p static pressure, N/m^2 (lbf/ft^2)

$q_j(\eta)$ coefficient of the jth chordal loading function, N/m (lbf/ft); j = 0 to N

q_∞ free-stream dynamic pressure, $\rho_\infty V_\infty^2/2$, N/m^2 (lbf/ft^2)

S actual wing area, m^2 (ft^2)

$V_N = V_\infty \cos \Lambda_{c/2}$, m/sec (ft/sec)

V_∞ free-stream velocity, m/sec (ft/sec)

w	perturbation velocity in z-direction, m/sec (ft/sec)
x,y,z	right-hand Cartesian coordinate system with origin in plane of symmetry at wing root midchord, m (ft) (see fig. 1)
x'	dummy variable form of x, m (ft)
ϵ	wing twist angle, rad (deg)
η	dimensionless spanwise coordinate, $\frac{y}{b/2}$
θ	chordwise angular location of ΔC_p, rad (deg)
$\Lambda_{c/2}$	sweep of midchord line on outboard portion of wing, rad (deg) (see fig. 1)
ρ_∞	free-stream density, kg/m^3 ($slugs/ft^3$)
ϕ	perturbation velocity potential, m^2/sec (ft^2/sec)

Subscripts:

LE	leading edge
TE	trailing edge

Mathematical symbols:

$[\,]$	square matrix
$\{\,\}$	column matrix

BASIC CONCEPTS

The transonic equivalence rule outlined by Spreiter and Stahara (ref. 4) states that the flow near a lifting slender-wing body at transonic speeds is the sum of two simpler flows. These simpler flows are the axisymmetric transonic flow over the equivalent body of revolution and the two-dimensional incompressible cross flow which will make the flow tangent to the surface. (See refs. 4 and 5.) Spreiter and Stahara point out that the loading on the wing, that is, the difference in pressure across the wing, depends only on the cross-

flow solution and can be calculated by linear theory even at transonic speeds. Since wing twist distribution depends mainly on the spanwise load distribution, the equivalence rule therefore indicates the possibility of designing the twist of a sonic aircraft wing by use of linear theory.

The same type of approach is not valid for the design of transonic airfoils. Linear theory indicates that the airfoil can be separated into thickness and camber, and that the same camber with different thickness distributions results in the same net pressure loading. These results are clearly incorrect in the nonlinear transonic range.

A linear theory has been used by Igoe (ref. 10) to calculate the twist distribution required for cruise near sonic speeds. Igoe found good agreement between the prediction of the theory and an experimentally determined twist of a supercritical wing, designed for low drag and high drag-divergence Mach number so as to result in efficient cruise near $M_\infty = 1$. Igoe used an expression for the downwash from reference 11 which applies to a wing of arbitrary aspect ratio at $M_\infty = 1$. However, the expression also agrees with results of slender-wing theory (slender or low-aspect-ratio wings at arbitrary Mach number). This agreement is not surprising because as M_∞ approaches 1.0, the Prandtl-Glauert correction continually reduces the aspect ratio. Hence, a high-aspect-ratio wing mathematically reduces to a slender wing as M_∞ approaches 1.0. Both cases, the high-aspect-ratio wing at $M_\infty = 1$ and the low-aspect-ratio or highly swept wing at arbitrary Mach number, are three-dimensional problems whose solutions can be obtained from the two-dimensional equation (discussed in refs. 11 and 12)

$$\frac{\partial^2 \phi}{\partial y^2} + \frac{\partial^2 \phi}{\partial z^2} = 0 \tag{1}$$

In the method of reference 10, the downwash at a given point on the wing is obtained by integrating over the area of the wing defined by the Mach forecone which is a plane at $M_\infty = 1$. The downwash is twice the value of the near-wake downwash from the portion of the wing forward of the given point; this is due to the fact that the Prandtl-Glauert transformation moves the point into the far wake of the forward part of the wing.

The present study utilizes the modified Multhopp lifting-surface theory for subsonic flow according to Lamar (ref. 13). This method of solving the downwash equations of lifting-surface theory (eq. (7-28) of ref. 5) uses a series representation of the pressure loading ΔC_p of the form[2]

---

[2]Reference 13 uses c for chord and $c(\eta)$ for half-chord. In the present report $c \equiv c(\eta)$.

$$\Delta C_p(\theta,\eta) = \frac{2}{c(\eta)}\left[\frac{q_0(\eta)}{q_\infty}\cot\frac{\theta}{2} + \sum_{j=1}^{N}\frac{q_j(\eta)}{q_\infty}\sin j\theta\right] \tag{2}$$

where $q_j(\eta)$ is the coefficient of the jth chordal loading function and θ and η are the chordwise and spanwise variables, respectively. The number of unknown pressure modes is $N + 1$.

Setting the leading-edge singularity to zero ($q_0 = 0$) yields a sine series for the chordwise load at η. In the present study, it was found that most practical loadings could be represented by a sine series. In this case the section load becomes

$$c_l(\eta)\, c(\eta) = \frac{\pi}{2}\frac{q_1(\eta)}{q_\infty} \tag{3}$$

By assuming an elliptic spanwise load to minimize induced drag, and using the relation for the total wing lift

$$C_L = \int_0^1 \frac{c_l(\eta)\, c(\eta)}{c_{av}}\, d\eta \tag{4}$$

the $q_1(\eta)/q_\infty$ coefficient can be written as

$$\frac{q_1(\eta)}{q_\infty} = \frac{8}{\pi^2} c_{av} C_L \sqrt{1 - \eta^2} \tag{5}$$

Determining the wing twist distribution involves what is referred to as the design problem. In the design problem the chordwise and spanwise load distributions, the planform, the design lift coefficient, and the cruise Mach number are specified. Once the shape of the chordwise load at η is selected, the coefficients $q_j(\eta)/q_1(\eta)$ can be calculated by a Fourier sine-series analysis. If the planform and the design lift coefficient C_L are known, the value of $q_1(\eta)/q_\infty$ can be computed from equation (5), and then each of the $q_j(\eta)/q_\infty$ coefficients can be computed.

The downwash at point (x,y) on the planform is then computed from the matrix equation

$$\left\{\frac{w(x,y)}{V_\infty}\right\} = \left[A^j(x,y,\eta)\right]\left\{\frac{q_j(\eta)}{q_\infty}\right\} \tag{6}$$

where the $A^j(x,y,\eta)$'s are elements of the influence coefficient matrix for computing the downwash at (x,y) caused by the jth chordal loading function at η. The elements $A^j(x,y,\eta)$ are functions of the planform shape and cruise Mach number. (See ref. 13.) Once the downwash is known, the shape of the mean camber surface is found from

$$\frac{z}{c} = \int_{(x/c)_{TE}}^{x/c} \left(\frac{w}{V_\infty}\right) d\left(\frac{x'}{c}\right) \tag{7}$$

where z/c is computed for the point x/c.

The twist angle ϵ at each span station is then computed from

$$\tan \epsilon = \left(\frac{z}{c}\right)_{LE} - \left(\frac{z}{c}\right)_{TE}$$

Since $(z/c)_{TE} = 0$ in reference 13, then

$$\epsilon = \tan^{-1}\left(\frac{z}{c}\right)_{LE}$$

In order to be consistent with the approximations of linear theory, it is assumed that

$$\left(\frac{z}{c}\right)_{LE} = \tan \epsilon \approx \epsilon \tag{8}$$

From equations (7) and (8) it is seen that the angle of twist is approximately proportional to the downwash velocity. It is also seen from the preceding results that the downwash velocity is directly proportional to the wing lift coefficient. Thus, once the loading, the planform shape, and the Mach number are fixed, the magnitude of ϵ varies linearly with the magnitude of C_L, and the value of ϵ/C_L at each span station is independent of the magnitude of C_L. This approximation was used in the calculations.

RESULTS AND DISCUSSION

Figure 1 and table I describe the wing planforms analyzed in this study. The number of chordwise control points, which also equals the number of chordwise pressure modes,[3] was 8; the number of spanwise stations on a semispan at which control points were located was 12 (includes station at wing center line).

Figure 2 shows the twist distribution of the 40° wing as calculated by lifting-surface theory for various values of the free-stream Mach number; also shown is the twist calculated by using slender-wing theory, as presented in figure 7 of reference 10. Since the twist is proportional to the wing lift, the twist angle has been divided by the wing lift coefficient. As shown in the sketch in the figure, the planform is approximated by

---

[3]Control points are locations where the tangent flow condition is satisfied; pressure modes are the trigonometric terms of equation (2).

straight line segments. Elliptic spanwise and rectangular chordwise loads were imposed for both solutions.

It is seen that as M_∞ approaches 1.0, the lifting-surface solution approaches the slender-wing solution, and for $M_\infty = 0.9999$, the lifting-surface solution is identical to the slender-wing solution outboard of $\eta = 0.5$. This is to be expected since, as explained previously, the transformed (equivalent incompressible) wing becomes very slender as M_∞ approaches 1.0. The areas of integration of the wing loading used to obtain the downwash at a given point on the wing also become equal for the two methods. The slender-wing solution integrates over the portion of the wing ahead of a given point. The lifting-surface solution integrates over the entire wing surface; however, the portion of the wing surface downstream of the given point has no influence on that point. This lack of influence can be seen by imagining that the downstream region of the wing is represented by, for example, a horseshoe vortex lattice. Infinitely far downstream of a horseshoe vortex, the induced downwash approaches a constant value. However, infinitely far upstream of a horseshoe vortex, the induced velocity goes to 0 (ref. 14). Since a horseshoe vortex downstream of a given point on the wing will be moved infinitely far downstream from the point on the transformed wing as M_∞ approaches 1.0, the vortex will not influence the given point.

Figure 2 shows that the net twist increases as M_∞ increases. This result can be explained by recalling that the angle of twist is directly proportional to the downwash velocity. As M_∞ increases, the transformed wing sweep increases, and points on the wing are swept farther into the wake of the more forward points, and therefore encounter greater downwash. The dip in the twist distribution in figure 2 between η of 0.2 and 0.4 is caused by the crank in the leading edge at $\eta = 0.266$.

Figure 3 compares the twist distribution from the lifting-surface theory with an experimentally determined twist distribution at $M_\infty = 1.00$. The calculations were made on the exact planform shape of the 40° wing (table I). An elliptic spanwise load distribution was used because the experimental spanwise load was very close to elliptic. Calculations were made for a rectangular chordwise load distribution and for the experimental chordwise load distributions that occurred near the design cruise condition. Two representatative experimental chordwise loads are shown in figure 4 with the Fourier sine series used to approximate them.

The experimental twist distribution in figure 3 was obtained from figure 7 of reference 10. These data were determined by model measurements which were corrected for wing incidence, angle of attack, and aeroelastic effects caused by bending. This wing was designed for low drag and high drag-divergence Mach number so as to result in efficient cruise near $M_\infty = 1$. At transonic speeds it is difficult to design a wing to maintain an elliptic span load because of the requirement for high lift coefficients at the tip. However,

as seen from reference 10, the experimental spanwise load distribution was very close to elliptic.

From figure 3 it is seen that the theory predicts the approximate magnitude and distribution of twist. The absence of the effects of the fuselage and the assumption of small perturbations in the calculations could account for the small discrepancies between the theory and the experiment.

The three planforms described in table I and figure 1 were used to determine the effect of sweep on the twist distribution. As indicated in figure 1, the planform variations occurred primarily on the portion of the wing outboard of the glove. Assuming that a quasi-two-dimensional flow exists over most of the wing, simple-sweep theory was used to define the cruise Mach numbers and the wing lift coefficients for the 36.5° and 31° wings. Because of the difficulty of maintaining two-dimensional flow over the entire span of a swept wing, it is not expected that the full benefit of sweep, as predicted by simple-sweep (cosine) theory, would be obtained. However, unpublished data from wind-tunnel tests by the Langley Research Center on carefully designed wing-body combinations have indicated that sweep benefits on drag-rise Mach number as large as $1/\cos^{0.8}\Lambda_{c/2}$ can be realized. Thus the normal component of Mach number was defined as

$$M_N = M_\infty \cos^{0.8}\Lambda_{c/2} \tag{9}$$

where $\Lambda_{c/2}$ is the sweep of the midchord line on the outboard section. The wing lift coefficient based on the normal component of free-stream velocity $C_{L,N}$ was calculated from the usual simple-sweep theory relation

$$C_L = C_{L,N} \cos^2\Lambda_{c/2} \tag{10}$$

Equations (9) and (10) were used to define the conditions for two cases. In the first case, the wing lift coefficient and normal component of Mach number were held constant; in the second case, both the lift coefficient based on the normal component of free-stream velocity and the normal component of Mach number were held constant. The latter case was an attempt to maintain the same sectional properties (based on V_N) over most of the span as the sweep was changed. (See ref. 15.)

Results for the first case are shown in figure 5. The lift coefficient was held constant at 0.31. By assuming a cruise Mach number of 0.9999 for the 40° wing, the normal component of Mach number was held constant and the cruise Mach numbers were calculated from equation (9) for the 36.5° and 31° wings. The experimental chordwise load distributions used in figure 3 and an elliptic spanwise load were used. Figure 5 indicates that significantly less twist is required as the sweep angle and Mach number are lowered. (The effect of Mach number alone is seen in fig. 2.)

Results for the second case are shown in figure 6. The wing lift coefficients required to maintain the airfoil near its design lift condition were determined from equation (10) with $C_{L,N}$ held constant. The Mach numbers and load distributions of figure 5 were used. Figure 6 shows that the effect of reduced Mach number and sweep angle is offset by the effect of an increase in the lift coefficient; thus, there is very little difference in the twist for the three wings. The contrasting effects of lift coefficient and Mach number are consistent with the results of figure 2.

Finally, it is useful to identify which factors primarily influence the wing twist. As seen from the preceding discussion, the wing twist for efficient cruise is determined by the planform shape, the cruise Mach number, the design lift coefficient, and the spanwise and chordwise load distributions. The effect of a large change in the shape of the chordwise load distribution on the twist of the 40° wing at a Mach number of 0.9999 is shown in figure 7. It is seen here, and also in figure 3, that for this planform the effect of large changes in the shape of the chordwise load distribution is small. Hence, for the cases investigated, if the span load is constrained to be elliptic, a family of twist distributions can be generated for a given planform which would apply to a reasonable range of chord loads. If it is assumed that $\tan \epsilon \approx \epsilon$ and the twist is generated in terms of ϵ/C_L for different span stations, the single parameter of this family would be M_∞. A series of curves such as those in figure 2 would result.

CONCLUSIONS

The transonic equivalence rule shows that chordwise and spanwise load distributions can be calculated on lifting wing bodies at transonic speeds using linear theory. Since wing twist distribution depends mainly on the spanwise load distribution, the equivalence rule therefore indicates the possibility of designing the twist of a sonic aircraft wing by use of linear theory.

As the free-stream Mach number approaches 1.0, the wing twist calculated by linear subsonic lifting-surface theory approaches the result calculated by slender-wing theory.

Linear lifting-surface theory was compared with experimental results on a high-aspect-ratio wing at transonic cruise conditions. The comparison showed that the theory predicts the approximate magnitude of the wing twist distribution required to maintain an elliptic span load for these conditions.

When the lift coefficient and component of Mach number normal to the outboard midchord line were held constant, variations in the sweep of the portion of a high-aspect-ratio wing outboard of the glove were found to require moderate changes in the twist distribution at transonic speeds. However, if both the normal Mach number and the lift coefficient based on the component of free-stream velocity normal to the outboard midchord line are

held constant, as suggested by simple-sweep theory, it was found that only small changes occur in the twist distribution.

For a given planform and an elliptic span load distribution, a single parameter family of twist distributions can be developed. This family is applicable to a reasonable range of chord load distributions and a lift coefficient low enough to insure that the tangent of the twist angle can be approximated by the angle itself. The family results from a plot of the twist angle divided by wing lift coefficient against spanwise location, with the cruise Mach number as a parameter.

Langley Research Center,
National Aeronautics and Space Administration,
Hampton, Va., October 8, 1974.

REFERENCES

1. Polhamus, Edward C.: Subsonic and Transonic Aerodynamic Research. Vehicle Technology for Civil Aviation – The Seventies and Beyond, NASA SP-292, 1971, pp. 27-44.

2. Bailey, F. R.; and Steger, J. L.: Relaxation Techniques for Three-Dimensional Transonic Flow About Wings. AIAA Paper No. 72-189, Jan. 1972.

3. Ballhaus, W. F.; and Bailey, F. R.: Numerical Calculation of Transonic Flow About Swept Wings. AIAA Paper No. 72-677, June 1972.

4. Spreiter, J. R.; and Stahara, S. S.: Calculative Techniques for Transonic Flows About Certain Classes of Airfoils and Slender Bodies. NASA CR-1722, 1971.

5. Ashley, Holt; and Landahl, Marten: Aerodynamics of Wings and Bodies. Addison-Wesley Pub. Co., Inc., c.1965.

6. Barnwell, R. W.: Transonic Flow About Lifting Wing-Body Combinations. AIAA Paper No. 74-185, Jan.-Feb. 1974.

7. Cheng, H. K.; and Hafez, M. M.: Equivalence Rule and Transonic Flow Theory Involving Lift. AIAA J., vol. 11, no. 8, Aug. 1973, pp. 1210-1212.

8. Lock, R. C.; and Rogers, E. W. E.: Aerodynamic Design of Swept Wings and Bodies for Transonic Speeds. Vol. 3 of Advances in Aeronautical Sciences, Pergamon Press, Inc., 1961, pp. 253-275.

9. Lock, R. C.: Some Experiments on the Design of Swept Wing Body Combinations at Transonic Speeds. Symposium Transsonicum, Klaus Oswatitsch, ed., Springer-Verlag, 1964, pp. 276-287.

10. Igoe, William B.: Calculation of Camber Using Slender Wing Theory at Mach Number 1.0. NASA TM X-2311, 1971.

11. Heaslet, Max. A.; Lomax, Harvard; and Spreiter, John R.: Linearized Compressible-Flow Theory for Sonic Flight Speeds. NACA Rep. 956, 1950.

12. Jones, Robert T.; and Cohen, Doris: Aerodynamics of Wings at High Speeds. Vol. VII of High Speed Aerodynamics and Jet Propulsion, A. F. Donovan and H. R. Lawrence, eds., Princeton Univ. Press, 1957, pp. 50, 97-107.

13. Lamar, John E.: A Modified Multhopp Approach for Predicting Lifting Pressures and Camber Shape for Composite Planforms in Subsonic Flow. NASA TN D-4427, 1968.

14. Milne-Thomson, L. M.: Theoretical Aerodynamics. Fourth ed., St. Martin's Press, Inc., 1966.

15. Rogers, E. W. E.; and Hall, I. M.: An Introduction to the Flow About Plane Swept-Back Wings At Transonic Speeds. J. Roy. Aeronaut. Soc., vol. 64, no. 596, Aug. 1960, pp. 449-464.

TABLE I.- PLANFORM COORDINATES

[Sweep angle refers to sweep of midchord line of the outboard portion of wing]

(a) 40^{o} swept planform; $c_{av}/(b/2) = 0.3860$

η	$\frac{x_{midchord}}{b/2}$	c/b
0	0	0.5602
.13053	.2111	.3549
.25882	.4013	.2051
.38268	.5209	.1642
.50000	.6191	.1473
.60876	.7102	.1327
.70711	.7929	.1196
.79335	.8658	.1076
.86603	.9271	.0978
.92388	.9756	.0902
.96593	1.0107	.0844
.99144	1.0320	.0807

TABLE I.- PLANFORM COORDINATES – Continued

(b) 36.5° swept planform; $c_{av}/(b/2) = 0.3511$

η	$\frac{x_{midchord}}{b/2}$	c/b
0	0	0.5438
.13053	.2092	.3399
.25882	.4012	.1898
.38268	.5142	.1506
.50000	.5988	.1359
.60876	.6794	.1229
.70711	.7519	.1100
.79335	.8153	.0992
.86603	.8692	.0906
.92388	.9115	.0830
.96593	.9426	.0779
.99144	.9611	.0746

TABLE I.- PLANFORM COORDINATES – Concluded

(c) 31^{o} swept planform; $c_{av}/(b/2) = 0.3085$

η	$\frac{x_{midchord}}{b/2}$	c/b
0	0	0.5221
.13053	.2046	.3241
.25882	.3989	.1649
.38268	.4908	.1336
.50000	.5604	.1207
.60876	.6275	.1094
.70711	.6859	.0982
.79335	.7373	.0886
.86603	.7804	.0808
.92388	.8160	.0741
.96593	.8409	.0700
.99144	.8562	.0671

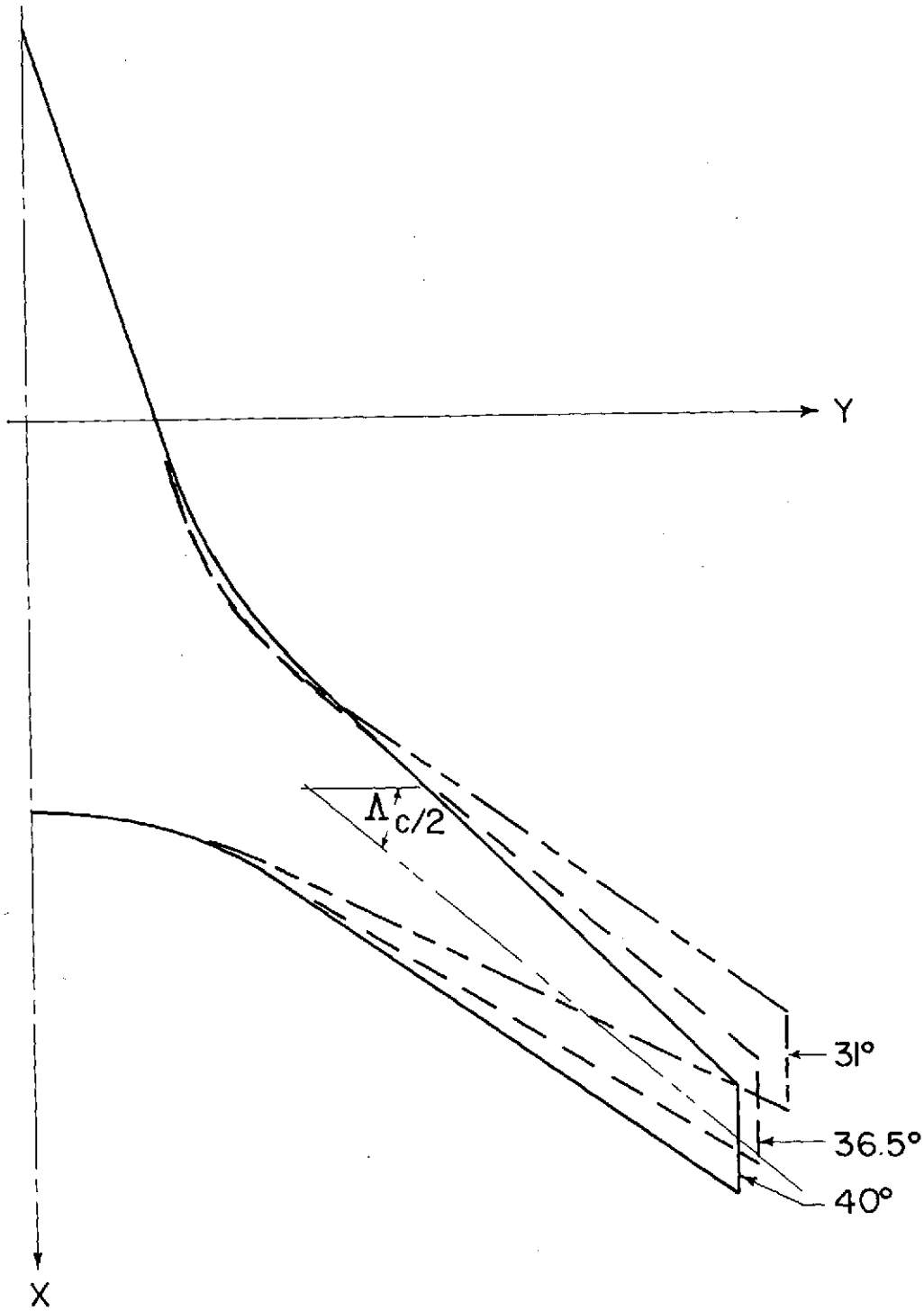

Figure 1.- General planforms and coordinate system. Sweep angles are given for the midchord line of the outboard panels.

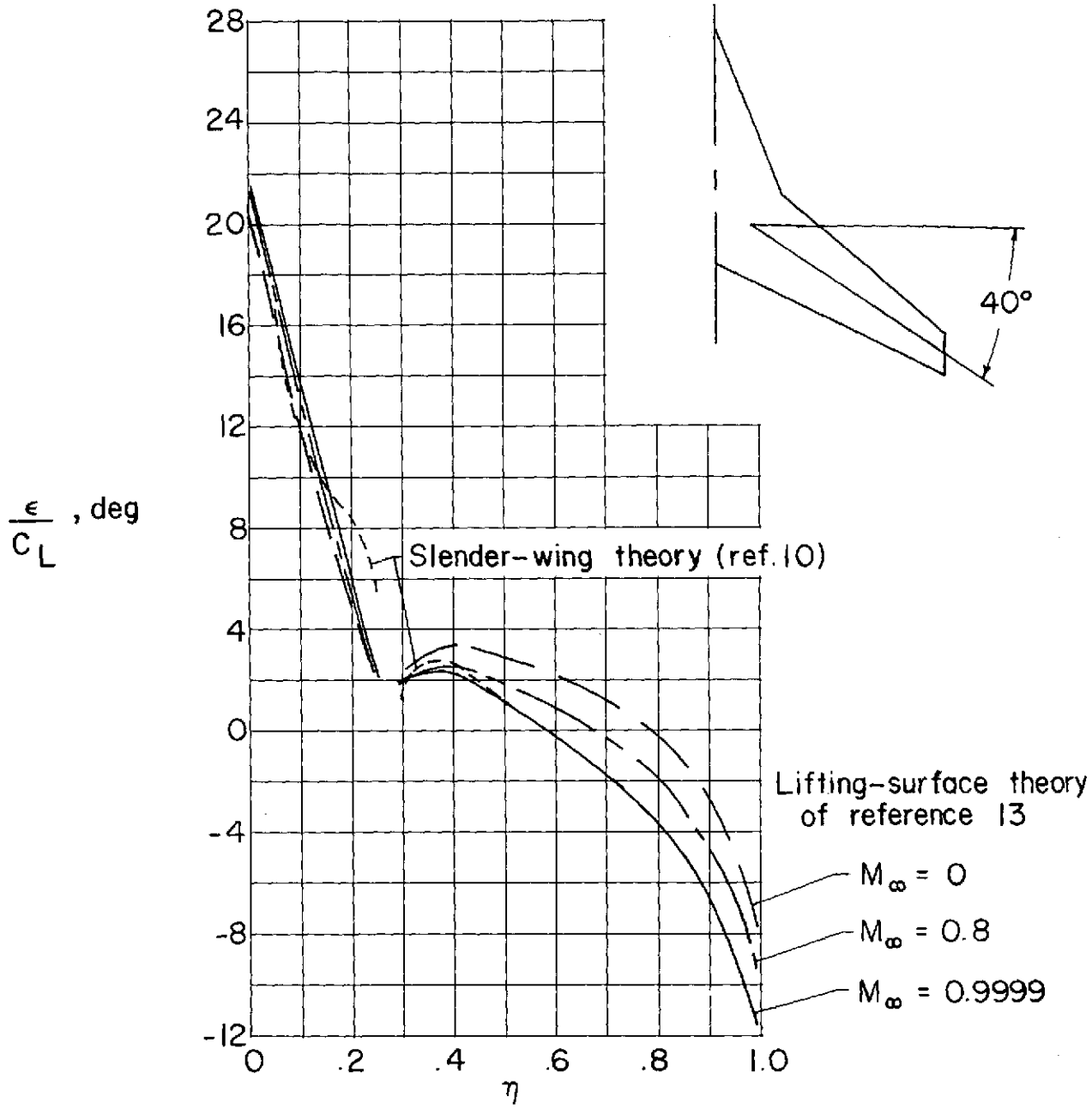

Figure 2.- Wing twist according to lifting-surface theory and slender-wing theory with elliptic spanwise and rectangular chordwise loads.

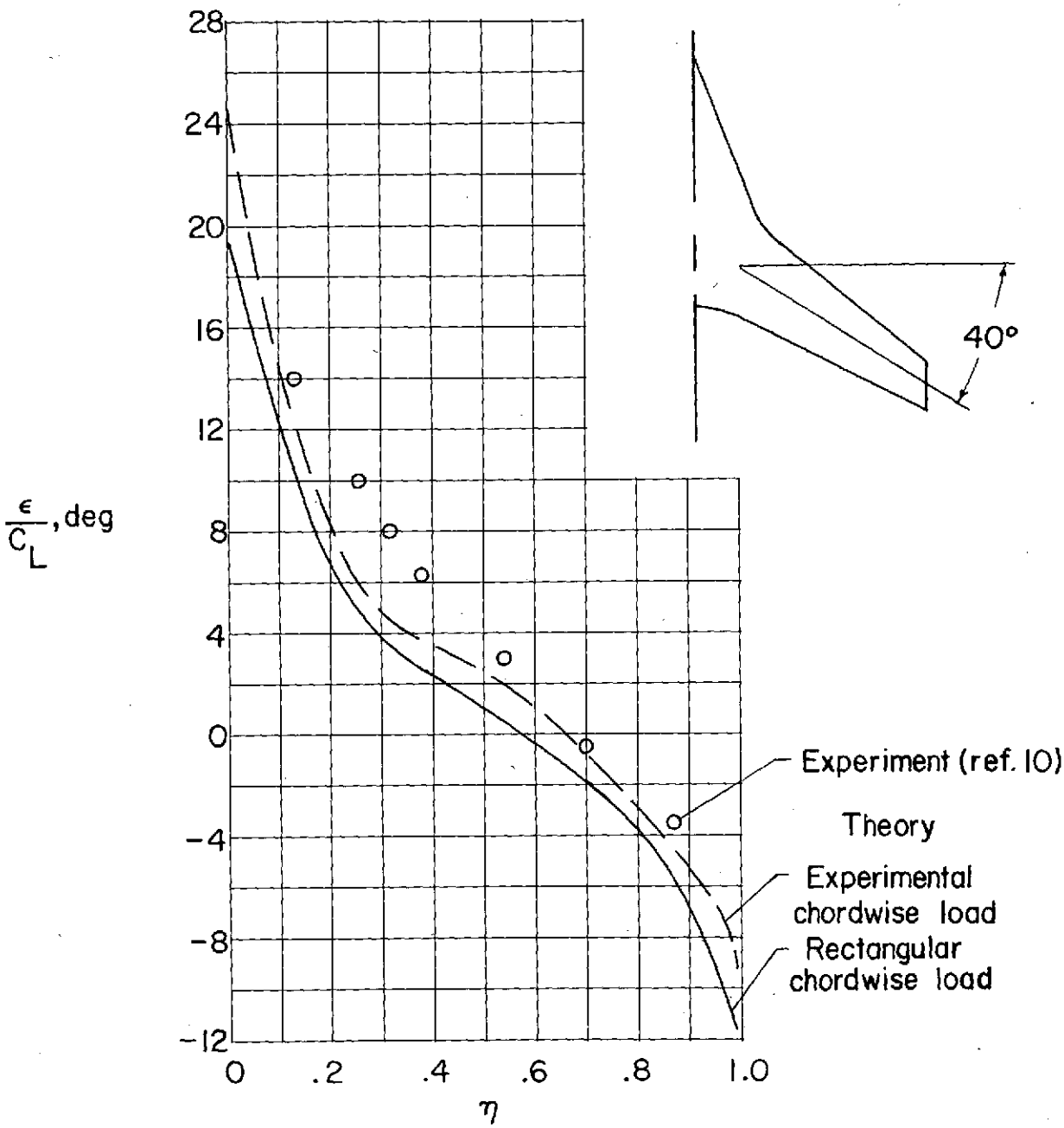

Figure 3.- Comparison of wing twist calculated by lifting-surface theory of reference 13 with experimental results at $M_\infty = 1.00$. Theory assumes an elliptic spanwise load.

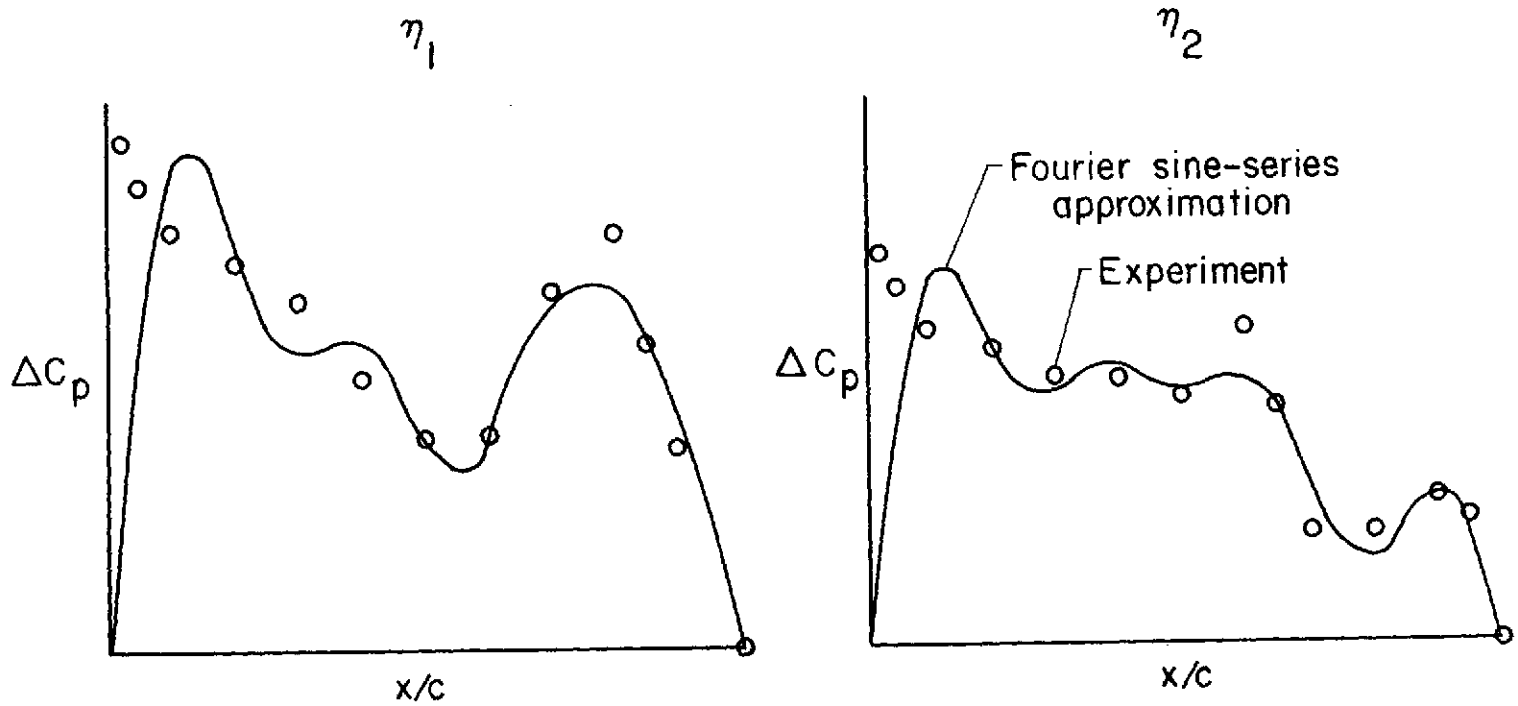

Figure 4.- Representative experimental chordwise loads at two span stations on the 40^o swept wing at $M_\infty = 0.99$ and the design lift coefficient with their Fourier sine-series approximation.

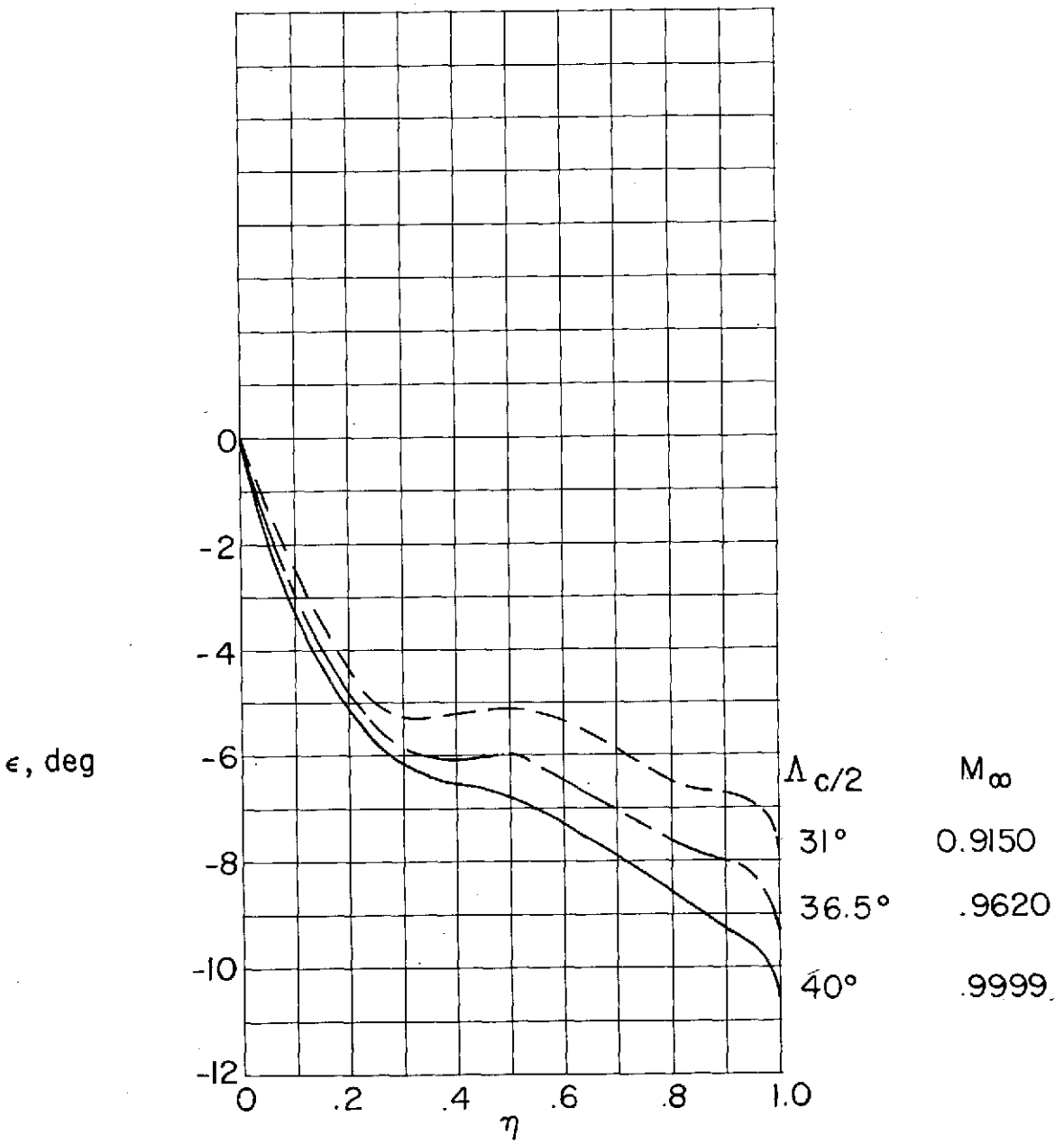

Figure 5.- Sweep effect on wing twist according to lifting-surface theory of reference 13 with M_N and C_L held constant ($C_L = 0.31$). Experimental chordwise load of 40^o wing and elliptic spanwise load.

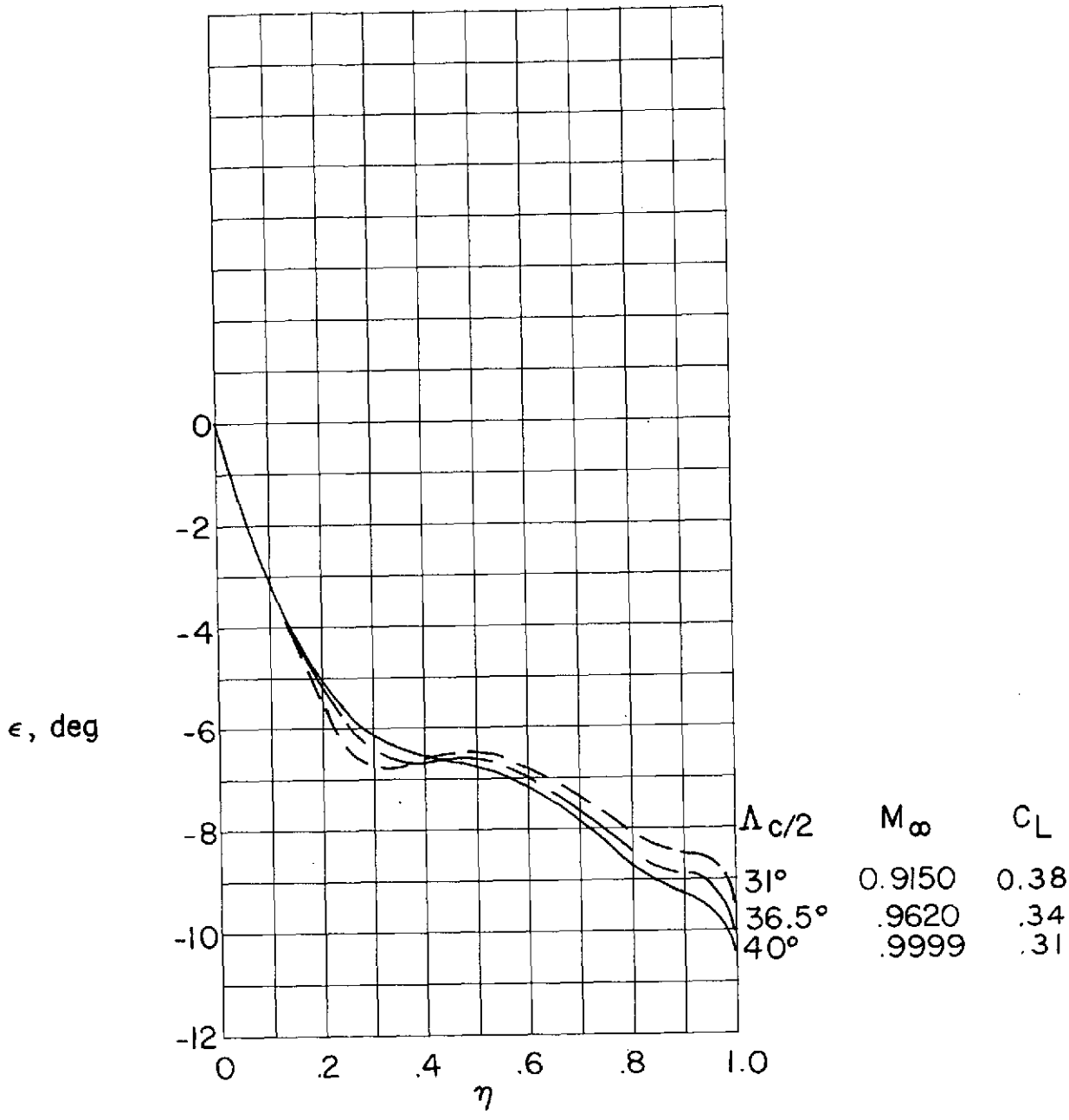

Figure 6.- Sweep effect on wing twist according to lifting-surface theory of reference 13 with M_N and $C_{L,N}$ held constant. Experimental chordwise load of 40^o wing and elliptic spanwise load.

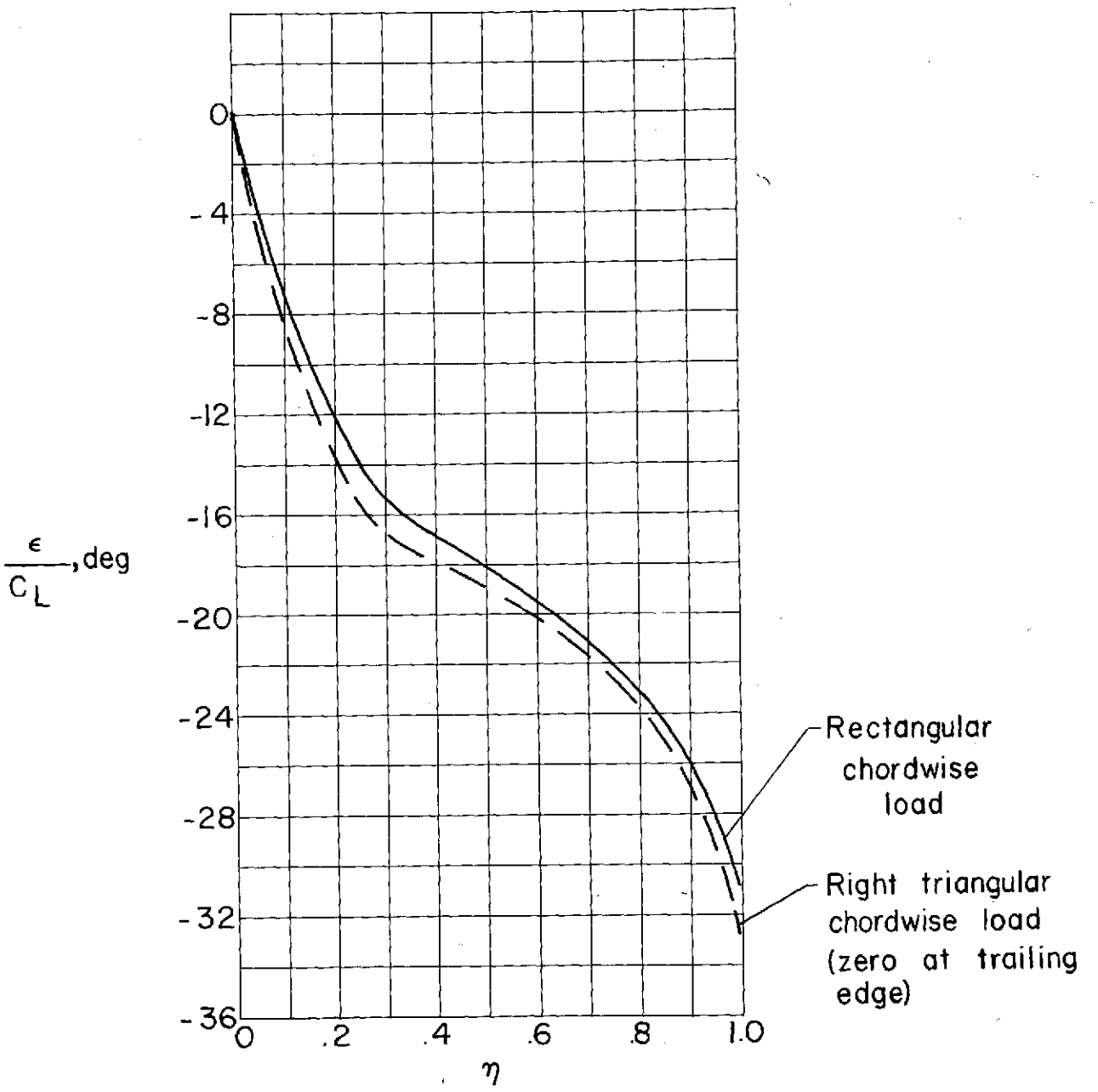

Figure 7.- Chordwise load effect on wing twist according to lifting-surface theory of reference 13 on the 40° swept wing at $M_\infty = 0.9999$. Elliptic spanwise load.